DOI: 10.17277/amt.2016.02.pp.008-015

Thermodynamic Properties of Multicomponent Amorphous Alloys in Fe–Si–B–Ni and Fe–Si–B–Ni–Co–Cr–Mo Systems

B.B. Khina[a]*, G.G. Goranskiy[b]

[a] *Physico-Technical Institute, National Academy of Sciences of Belarus, 10 Kuprevich Street, Minsk 220141, Belarus*
[b] *Scientific and Technological Park "Polytechnic", Belorussian National Technical University, 65 Nezavisimosti Avenue, Minsk 220027, Belarus*

* Corresponding author: Tel.: + 3 (7529) 3029387. *E-mail*: khina_brs@mail.ru

Abstract

The chemical potential of iron in a amorphous phase of multicomponent multiphase alloys Fe – 7.3 % Si – 14.2 % B – 8.26 % Ni (alloy 1) and Fe – 0.32 % Si – 4.8 % B – 6.68 % Ni – 2.42 % Co – 8.88 % Cr – 6.42 % Mo (alloy 2), which contain crystalline and amorphous phases, was determined on the basis of experimental results and a theoretical model. The alloys were produced by melt quenching at a cooling rate of the order of 10^5 K/s and subsequent mechanical milling in an attritor, which resulted in an increase in the fraction of the amorphous phase and improvement of its thermal stability. The chemical potential of iron in a non-equilibrium alloy containing an amorphous phase and crystalline phases (iron-base α-solid solution, FeB, Fe_2B, FeSi and other compounds) was determined by an electrochemical method. In order to define the chemical potential of iron in the amorphous phase from the results of electrochemical measurements, a thermodynamic model was developed using the CALPHAD approach for crystalline phases and the SGTE database for pure elements. To evaluate the enthalpy and entropy contribution to the chemical potential of Fe in amorphous phases, the theory of mismatch entropy was employed. It is found that milling in the attritor improves the stability of multicomponent amorphous phases in the above systems, which can be attributed to changes in the cluster-atomic structure of an amorphous phase due to intensive plastic deformation.

Keywords

Amorphous alloys; CALPHAD approach; chemical potential; mismatch entropy; partial molar enthalpy; partial molar entropy.

Introduction

Amorphous alloys, or metallic glasses are currently used in industry as materials and coatings for a wide range of applications due to their unique features, e.g., high elastic properties, good corrosion stability in many environments, low friction coefficient, etc. [1]. Also, crystallization of metallic glasses at heating above crystallization temperature T_{cr} can be used for producing crystalline alloys with fine grains the size of which ranges from submicro- to nano-level [2]. Typically, thermodynamic properties of amorphous alloys, namely the formation enthalpy, are estimated using semi-empirical Miedema model [3], which is also employed for evaluating the glass-forming ability of multicomponent liquids. However, the thermodynamic stability of phases is determined by the Gibbs energy rather than by enthalpy. A comparison of thermodynamic properties of amorphous phases with experimental data has not been performed yet either. Direct evaluation of the Gibbs energy from experimental data is very difficult but it is possible to measure the chemical potential, i.e. partial molar free energy, of a base metal of amorphous alloy using electrochemical method [4, 5].

Recently, economically alloyed iron-base compositions in the Fe–Si–B–Ni and Fe–Si–B–Ni–Co–Cr–Mo systems have been developed at the Belorussian National Technical University for producing amorphous and crystalline-amorphous materials and coatings. The problem is that at rapid cooling using the melt spinning method the liquid alloys do not amorphize completely because of a large difference in cooling rates on the opposite sides of the

obtained ribbon. For a multiphase amorphous-crystalline alloy, the physical meaning of the data obtained by electrochemical measurements is not clear.

Thus, the objective of this work is to develop a theoretical method for evaluating the thermodynamic properties of an amorphous phase, namely the chemical potential of iron, in the given systems on the basis of experimental measurements. This will permit estimating, in thermodynamic terms, a difference between amorphous phases produced by different methods, e.g., melt quenching and mechanical alloying.

Experimental Methods and Materials

Rapidly quenched alloys with overall compositions (wt.%) Fe – 7.3 % Si–14.2 % B – 8.26 % Ni (alloy 1) and Fe – 6.68 % Ni – 6.42 % Mo – 8.88 % Cr – 2.42 % Co – 0.32 % Si – 4.8 % B (alloy 2) were produced by melt spinning using a rotating water-cooled copper drum. The cooling rate was $2.5 \cdot 10^5$ K/s for alloy 1 and $4 \cdot 10^5$ K/s for alloy 2. The phase compositions of thus obtained ribbons were studied by X-ray diffraction (**XRD**) analysis using DRON-3 diffractometer in monochromated Cu-K_α radiation. To provide more complete amorphization of the alloys, the ribbons were crushed into powder and subjected to intensive ball milling in an attritor with a vertical impeller whose rotating speed was varied from 3 to 20 s^{-1}. The volume of the working chamber of the attritor was 1 dm^3, the diameter of balls made from hard alloy VK6 (94 % tungsten carbide – 6 % Co, Russian National Standard GOST 3882-74) was 5 mm, the mass of the balls was up to 3 kg, the mass of powder was 30 g, the duration of attritor processing (AP), t, was 10 to 60 min. As a result of AP, the content of amorphous phase in the alloys increased up to 98 %.

After AP the alloy powders were studied by differential thermal analysis (**DTA**) to measure the temperature of the crystallization onset, T_{cr}, and adiabatic heating at crystallization, ΔT, using a Perkin Elmer TG/DTA system; heating was performed in helium at a rate of 2, 5 and 10 K/min.

To study thermodynamic properties of alloys, a difference of the chemical potential of iron, $\Delta\mu_{Fe}^{(exp)}$, between the multiphase iron-base alloy, which is used as anode, and a cathode made from pure α(bcc)-Fe was measured using an electrochemical method which was developed in [4, 5] for fully amorphous alloys. The method is based on detecting an instantaneous value of the electromotive force in a concentration-type electrochemical cell where a solution of sodium chloride and iron sulfate in pure alcohol is used as an electrolyte:

$$-\text{Fe} \mid \text{KCl}, \text{Fe}_2(\text{SO}_4)_3, \text{C}_2\text{H}_5\text{OH} \mid \langle\text{Fe}\rangle \text{ in alloy}+.$$

Experimental Results and Discussion

The experimental data obtained by XRD, electrochemical measurements and DTA analysis of alloys 1 and 2 in the as-quenched state (time of AP $t = 0$) and after AP are presented in Table 1. It is seen

Table 1

Experimental data: phase composition of alloys 1 and 2, difference of the chemical potential of iron, $\Delta\mu_{Fe}^{(exp)}$, between the multiphase alloy and pure α-Fe, temperature of the onset of crystallization, T_{cr}, and adiabatic heating, ΔT, at crystallization of an amorphous phase

Alloy	Milling time *t*, min	Phase composition, wt %							$\Delta\mu_{Fe}^{(ex)}$, J/mol	T_{cr}, K	ΔT, K
		amorphous	α-solid solution	σ-FeCr	λ-Fe_2Mo	Fe_2B	FeB	FeSi			
1	0	78	18	–	–	1	2	1	6122	703	220
	10	80	16	–	–	1	2	1	5814	736	246
	15	84	11	–	–	1	3	1	5623	752	265
	20	85	10	–	–	1	3	1	4820	765	265
	40	92	4	–	–	–	3	1	4606	785	340
	60	98	–	–	–	–	2	–	4012	785	355
2	0	82	12	3	2	1	–	–	4083	755	220
	10	82	12	3	2	1	–	–	3452	764	245
	15	86	10	2	1	1	–	–	3106	776	285
	20	88	9	1	1	1	–	–	2796	798	310
	40	96	1	1	1	1	–	–	2550	818	370
	60	98	–	–	1	1	–	–	2101	818	385

that for both alloys the cooling rate during melt spinning appeared insufficiently high to provide complete amorphization: the content of amorphous phases in the as-quenched state was 78 % for alloy 1 and 82 % for alloy 2. After AP the content of amorphous phase in both alloys reached 98 % because of dissolution of crystalline phases due to deformation-induced non-equilibrium diffusion, which is known to occur at mechanical alloying [6].

It is also seen that the thermal stability of the alloys is improved by AP: the temperature of the onset of crystallization T_{cr} and adiabatic heating ΔT have increased. The latter can be attributed to the increase in the content of amorphous phase, but the former can be connected with enhanced stability of an amorphous phase due to intensive shear deformation during AP. It is known [7] that amorphous alloys consist of clusters containing ~10 atoms and individual atoms positioned chaotically between them, and this cluster-atomic structure can change at annealing below T_{cr} (the so-called structural relaxation [1]) and during shear plastic deformation [7]. A decrease in the $\Delta\mu_{Fe}^{(exp)}$ values with increasing the milling time also testifies to the stability improvement of the amorphous phase. However, this parameter measured by the electrochemical method refers not to a single amorphous phase but to a composite amorphous-crystalline material.

Hence it is necessary to develop a thermodynamic method for determining the chemical potential of iron in an amorphous phase, $\mu_{Fe}^{(am)}$, and its partial molar enthalpy, $h_{Fe}^{(am)}$, from the experimental data obtained for a non-equilibrium multiphase alloy. Then it will be possible to evaluate quantitatively the effect of intensive plastic deformation during AP on the thermodynamic properties of a multicomponent amorphous phase and to link it, at least on a qualitative level, to changes in cluster-atomic structure and free volume of the amorphous phase.

Thermodynamic Model

Chemical potential in a non-equilibrium multiphase alloy

In a well-annealed multicomponent multiphase alloy, chemical potential of an element is the same throughout the volume, which follows from the condition of thermodynamic equilibrium. For a fully amorphous alloy, the variation of composition in the volume can be neglected, and chemical potential of a base metal in such an alloy can be considered constant at a given temperature, which forms a basis for electrochemical measurements performed in [4, 5]. In the considered amorphous-crystalline alloys, we deal with a substantially non-equilibrium situation. Drawing an analogy with the description of electrochemical reactions [8], we assume that effective chemical potential of *i*-th element in a non-equilibrium multiphase alloy, μ_i^{ef}, is a volume-averaged value:

$$\mu_i^{ef} = \sum_{\varphi=1}^{N} \mu_i^{(\varphi)} X_\varphi, \qquad (1)$$

where X_φ is the molar fraction of phase φ in the alloy and N is the total number of phases, $\sum_{\varphi=1}^{N} X_\varphi = 1$; we assign φ = 1 to amorphous phase.

Then the experimental parameter $\Delta\mu_{Fe}^{(ex)}$ has the following physical meaning:

$$\Delta\mu_{Fe}^{(exp)} = \mu_{Fe}^{ef} - G_{Fe}^{(\alpha)}, \qquad (2)$$

where $G_{Fe}^{(\alpha)}$ is the Gibbs energy of pure α-Fe, i.e. its chemical potential $\mu_{Fe}^{(\alpha)} \equiv G_{Fe}^{(\alpha)}$.

From (1) and (2) the chemical potential of Fe in the amorphous phase is determined as

$$\mu_{Fe}^{(am)} = \left(\Delta\mu_{Fe}^{(exp)} - \sum_{\varphi=2}^{N} \mu_{Fe}^{(\varphi)} X_\varphi + G_{Fe}^{(\alpha)} \right) \Big/ X_{am}. \qquad (3)$$

The molar fraction of phase φ in a multiphase alloy, X_φ, is connected with its mass fraction, C_φ:

$$X_\varphi = \frac{C_\varphi / m_\varphi}{\sum_{\varphi=1}^{N} C_\varphi / m_\varphi}, \quad m_\varphi = \sum_{\varphi=1}^{N} x_i^\varphi m_i,$$

$$\sum_{\varphi=1}^{N} c_i^\varphi C_\varphi = c_i^0, \quad \sum_{\varphi=1}^{N} x_i^\varphi X_\varphi = x_i^0, \qquad (4)$$

where m_φ is the molecular mass of phase φ, m_i is the atomic mass of *i*-th element, x_i^φ and c_i^φ are the molar and mass concentration of *i*-th element in phase φ, x_i^0 and c_i^0 are its overall molar and mass content in the multiphase alloy.

Then, to use formula (3), it is necessary to determine the chemical potential of Fe in all the crystalline phases (solid solutions and compounds) listed in Table 1.

Chemical potential of iron in crystalline phases

In multicomponent phase φ, partial molar parameters of *i*-th component $z_i^{(\varphi)} = \mu_i^{(\varphi)}$, $h_i^{(\varphi)}$, $s_i^{(\varphi)}$, $\Delta h_{\text{ex},i}^{(\varphi)}$ (chemical potential, partial enthalpy, partial entropy and partial excess enthalpy of mixing, respectively) are determined from the corresponding integral thermodynamic parameters of this phase, which are defined per one mole of solution $Z_\varphi = G_\varphi$, H_φ, S_φ, H_{ex}^φ (the Gibbs energy, enthalpy, entropy and excess enthalpy, respectively), according to the following equation [9]:

$$z_i^{(\varphi)} = Z_\varphi + \sum_{j=2}^{k} \left(\delta_{ij} - x_j\right) \frac{\partial Z_\varphi}{\partial x_j}, , \qquad (5)$$

where k is the number of components, $i = 1$ refers to the base element (here Fe), and δ_{ij} is the Kronecker delta: $\delta_{ij} = 1$ at $i = j$, $\delta_{ij} = 0$ at $i \neq j$.

Hereinafter we employ thermodynamic models for crystalline phases, which are used in the CALPHAD (Calculation of Phase Diagrams) approach [10]. The Gibbs energy of a multicomponent substitutional solid solution φ (here it is the iron-base α-phase) is described using the regular solution concept:

$$G_\varphi = \sum_{i=1}^{k} x_i^\varphi \mu_i^{(\varphi)} = \sum_{i=1}^{k} x_i^\varphi G_i^\varphi + G_{\text{mix, id}}^\varphi + G_{\text{ex}}^\varphi,$$

$$G_{\text{mix,id}}^\varphi = -TS_{\text{id}}^\varphi, \quad S_{id}^\varphi = -R\sum_{i=1}^{k} x_i^\varphi \ln x_i^\varphi, \qquad (6)$$

where G_i^φ is the Gibbs energy of *i*-th component in phase φ, G_{ex}^φ is the excess free energy of mixing (actually, enthalpy of mixing, $G_{\text{ex}}^\varphi = H_{\text{ex}}^\varphi$), $G_{\text{mix,id}}^\varphi$ is the ideal energy of mixing (the entropic term), S_{id}^φ is the ideal, or configurational entropy of mixing and R is the universal gas constant.

In the CALPHAD approach, the Gibbs energy of pure *i*-th component in phase φ is expressed in a polynomial form:

$$G_i^\varphi = a_i + b_i T + c_i T \ln T + \sum_n d_{i,n} T^n + \\ + H_i^{\text{SER}} + G_{i,\text{pres}}^\varphi + G_{i,\text{mag}}^\varphi. \qquad (7)$$

Here $G_{i,\text{pres}}^\varphi$ and $G_{i,\text{mag}}^\varphi$ describe the contribution of pressure and magnetic ordering to the total Gibbs energy of *i*-th element in phase state φ, H_i^{SER} is the so-called standard element reference, a_i, b_i, c_i and $d_{i,n}$ are numerical parameters for *i*-th element, and n is an integer. Parameter $H_i^{\text{SER}} = H_i(T=298) - H_i(T=0)$ has a meaning of a correction term when passing from $T = 298$ K to $T = 0$ K as a standard temperature for calculating G and H.

For most of the elements in different phase states, the values of parameters a, b, c, d and H_i^{SER} in Eq. (7), as well as formulas for calculating $G_{i,\text{pres}}^\varphi$ and $G_{i,\text{mag}}^\varphi$ for ferromagnetic and paramagnetic states, are presented in SGTE database [11].

The excess energy of mixing that appears in (6) is determined as

$$G_{\text{ex}}^\varphi = H_{\text{ex}}^\varphi = \sum_{i,j} x_i^\varphi x_j^\varphi L_{ij}^\varphi + \sum_{i,j,k} x_i^\varphi x_j^\varphi x_k^\varphi L_{ijk}^\varphi, \; i \neq j \neq k. \qquad (8)$$

Here L_{ij}^φ and L_{ijk}^φ, $i \neq j \neq k$, are the parameters of binary (*i*-*j*) and ternary (*i*-*j*-*k*) interaction in phase φ. They are described by a Redlich-Kister-Muggianu polynomial [10]. For binary interaction

$$L_{ij}^\varphi = \sum_n {}^n L_{ij}^\varphi \left(x_i^\varphi - x_j^\varphi\right)^n, \quad i \neq j, \quad n \geq 0, \qquad (9)$$

where n is a positive integer. For ternary interaction

$$L_{ijk}^\varphi = {}^0 L_{ijk}^\varphi + {}^i L_{ijk}^\varphi x_i^\varphi + {}^j L_{ijk}^\varphi x_j^\varphi + {}^k L_{ijk}^\varphi x_k^\varphi, \; i \neq j \neq k. \qquad (10)$$

The temperature dependence of parameters ${}^n L_{ij}^\varphi$, $n \geq 0$, and ${}^m L_{ijk}^\varphi$, $m = 0, i, j, k$, $i \neq j \neq k$, is typically considered as linear, $L = A + BT$.

In calculating the Gibbs energy of Fe-base α-solid solution according to formulas (8) – (10), the parameters for binary interactions Fe–Cr, Fe–Si, Cr–B, Cr–Ni, Cr–Si, Ni–B, Ni–Mo, Ni–Si и Mo–Si were taken from [12], for Fe–B, Fe–Co and Co–B from [13], for Fe–Ni from [14], for Fe–Mo from [15], and ternary interaction parameters Fe–Cr–Ni, Fe–Ni–Mo, Fe–Ni–Si were taken from [12]. The formulas for chemical potential of iron in alloys 1 and 2, which are derived by applying Eq. (5) to (6) and taking into account expressions (8) – (10), are too cumbersome and cannot be presented here.

The thermodynamics of binary compounds in the CALPHAD approach is described by the Hillert-Staffanson sublattice model [9, 10]. For rhombohedral phase Fe_2B per 1 mole of solution, i.e. for formula $Fe_{0.67}B_{0.33}$, we have [16]

$$G_{\text{Fe}_{0.67}\text{B}_{0.33}} = \left(2G_{\text{Fe}}^{\text{BCC}} + G_{\text{B}}^{\text{rho}} - 81226 + 3.01T\right)/3. \qquad (11)$$

Here $G_{\text{B}}^{\text{rho}}$ is the Gibbs energy of boron in a state with a rhombohedral lattice, $G_{\text{Fe}}^{\text{BCC}}$ is the Gibbs energy of α(bcc)-Fe [11].

Then, using Eq. (5), we obtain the chemical potential of Fe in Fe_2B:

$$\mu_{Fe}^{(Fe_2B)} = G_{Fe}^{BCC} - 27075 + 1.0033T. \quad (12)$$

For phase FeB per 1 mole, i.e. for $Fe_{0.5}B_{0.5}$, we have [16]:

$$G_{Fe_{0.5}B_{0.5}} = \left(G_{Fe}^{BCC} + G_{B}^{rho} - 73933 + 0.3076T\right)/2. \quad (13)$$

Using Eq. (5), we derive the chemical potential of Fe in FeB:

$$\mu_{Fe}^{(FeB)} = G_{Fe}^{FCC} - 36967 + 0.1538T. \quad (14)$$

Similarly, using data [17], we obtain the chemical potential of Fe in phase FeSi per 1 mole of solution (i.e. for $Fe_{0.5}Si_{0.5}$):

$$\mu_{Fe}^{(FeSi)} = G_{Fe}^{BCC} - 36381 + 2.22T. \quad (15)$$

For σ-FeCr phase, a three-sublattice model is used: it is represented as $(Fe)_8(Fe,Cr)_{18}(Cr)_4$ [18], and its Gibbs energy per 1 mole of solution looks as

$$G_{\sigma} = \left[y''_{Fe} G^{\sigma}_{Fe:Fe:Cr} + y''_{Cr} G^{\sigma}_{Fe:Cr:Cr} + \right.$$
$$\left. + 18RT\left(y''_{Fe}\ln y''_{Fe} + y''_{Cr}\ln y''_{Cr}\right)\right]/30, \quad (16)$$

where parameters $G^{\sigma}_{Fe:Fe:Cr}$ and $G^{\sigma}_{Fe:Cr:Cr}$ are defined as

$$G^{\sigma}_{Fe:Fe:Cr} = 8G_{Fe}^{FCC} + 18G_{Fe}^{hBCC} + 4G_{Cr}^{hBCC} + 72000 - 31T,$$
$$G^{\sigma}_{Fe:Cr:Cr} = 8G_{Fe}^{FCC} + 22G_{Cr}^{hBCC} + 49000 - 31T. \quad (17)$$

In (16) and (17), y'_{Fe} and y''_{Fe} are the site fractions of iron atoms in sublattices I and II, y'_{Cr} and y''_{Cr} are the same for chromium; G_{Fe}^{FCC} is the Gibbs energy of γ(fcc)-Fe, G_{Fe}^{hBCC} and G_{Cr}^{hBCC} are the Gibbs energy of iron in a hypothetical paramagnetic bcc state, which are determined from the SGTE database [11].

Assuming the composition of σ-phase as $Fe_{0.5}Cr_{0.5}$, for which $y''_{Fe} = 7/18$ and $y''_{Cr} = 11/18$, and applying Eq. (5) to (17), we obtain the chemical potential of Fe:

$$\mu_{Fe}^{(\sigma)} = \left(8G_{Fe}^{FCC} + 18G_{Fe}^{hBCC} + 4G_{Cr}^{hBCC} + \right.$$
$$\left. + 72000 - 31T + 18RT\ln\frac{7}{18}\right)/30. \quad (18)$$

In [15], phase λ-Fe_2Mo is described as a two-sublattice compound $(Fe,Mo)_2Mo_1$. Since it is the so-called linear compound, then $y'_{Mo} = 0$ and $y'_{Fe} = 1$. Considering 1 mole of solution, i.e. $Fe_{0.67}Mo_{0.33}$, and applying Eq. (5) to thermodynamic model [15], the chemical potential of Fe in this phase is obtained as

$$\mu_{Fe}^{(Fe_2Mo)} = G_{Fe}^{FCC} - 3599.3 + 0.044T. \quad (19)$$

Partial molar characteristics of iron in amorphous phase

After calculating the chemical potential of Fe in amorphous phase using Eq. (3) and the above presented formulas for μ_{Fe} in crystalline phases of a multiphase alloy, it becomes possible to determine the partial molar enthalpy $h_{Fe}^{(am)}$ and excess partial molar enthalpy $\Delta h_{ex,Fe}^{(am)}$ of iron using classical definitions [9, 10]:

$$\mu_{Fe}^{(am)} = h_{Fe}^{(am)} - Ts_{Fe}^{(am)} = G_{Fe}^{am} + \Delta h_{ex,Fe}^{(am)} - Ts_{Fe}^{(am)},$$
$$h_{Fe}^{(am)} = H_{Fe}^{am} + \Delta h_{ex,Fe}^{(am)}. \quad (20)$$

Here $s_{Fe}^{(am)}$ is the partial molar enthalpy of Fe in a multicomponent amorphous phase, G_{Fe}^{am} and H_{Fe}^{am} are the Gibbs energy and enthalpy, correspondingly, of pure Fe in amorphous state. According to [19], enthalpy of a pure element in amorphous state is the same as in supercooled liquid, i.e. $H_{Fe}^{am} = H_{Fe}^{liq}$ and $G_{Fe}^{am} = G_{Fe}^{liq}$.

Now it is necessary to determine the entropy term in formulas (20). For crystalline phases, as seen from (6), only the ideal entropy of mixing S_{id}^{φ} exists. In amorphous phase, along with S_{id}^{am} there is mismatch entropy S_{σ}^{am} which is due to a difference in atomic sizes [20, 21], i.e. $S_{am} = S_{id}^{am} + S_{\sigma}^{am}$. Then for partial molar entropy of iron in amorphous phase

$$s_{Fe}^{(am)} = S_{Fe}^{liq} + s_{id,Fe}^{(am)} + s_{\sigma,Fe}^{(am)}, \quad s_{id,Fe}^{(am)} = -R\ln x_{Fe}^{(am)}, \quad (21)$$

where $s_{\sigma,Fe}^{(am)}$ is the partial molar entropy of Fe in the amorphous phase and $S^{liq}_{Fe} = (H_{Fe}{}^{liq} - G_{Fe}{}^{liq})/T$ is the standard entropy of pure iron in the liquid state.

The mismatch entropy per 1 mole of solution is defined as [20, 21]

$$S_{\sigma}^{am} = R\left\{1.5\left(\zeta^2 - 1\right)y_1 + 1.5\left(\zeta - 1\right)^2 y_2 - \right.$$
$$\left. - \left[\left(\zeta - 1\right)\left(\zeta - 3\right)/2 + \ln\zeta\right]\left(1 - y_3\right)\right\}, \quad (22)$$

where $\zeta = 1/(1-\xi)$, $\xi = 0.64$ for dense packing of spherical particles; parameters y_2 and y_3 look as

$$y_1 = (1/\sigma_3) \sum_{j \geq i=1}^{k} \left(d_i + d_j\right)\left(d_i - d_j\right)^2 x_i x_j,$$

$$y_2 = \left(\sigma_2/\sigma_3^2\right) \sum_{j \geq i=1}^{k} d_i d_j \left(d_i - d_j\right)^2 x_i x_j,$$

$$y_3 = \sigma_2^3/\sigma_3^2, \quad \sigma_n = \sum_{i=1}^{k} x_i d_i^n, \quad n = 2, 3, \tag{23}$$

d_i and d_j being the diameters of i-th and j-th species, $i \neq j$.

Then the partial molar mismatch entropy of iron in amorphous phase, $s_{\sigma,\mathrm{Fe}}^{(\mathrm{am})}$, is determined by applying Eq. (5) to formulas (22) and (23); the derived expression is too cumbersome and therfore is not presented.

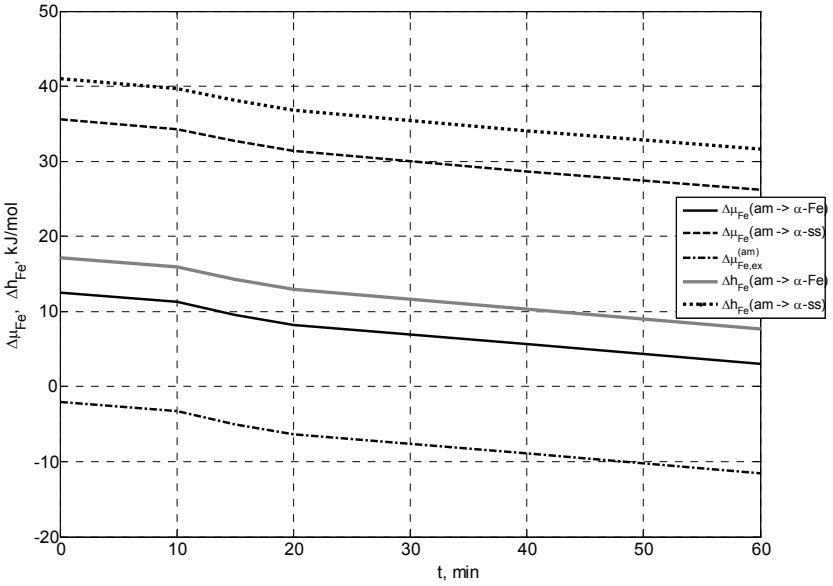

Fig. 2. Differences of partial molar thermodynamic parameters of iron in the amorphous phase of alloy 1 with regard to α-solid solution of the same composition $\left(\Delta\mu_{\mathrm{Fe}}^{(\mathrm{am}\to\alpha-\mathrm{ss})}\right.$ and $\left.\Delta h_{\mathrm{Fe}}^{(\mathrm{am}\to\alpha-\mathrm{ss})}\right)$, pure α-Fe $\left(\Delta\mu_{\mathrm{Fe}}^{(\mathrm{am}\to\alpha-\mathrm{Fe})}\right.$ and $\left.\Delta h_{\mathrm{Fe}}^{(\mathrm{am}\to\alpha-\mathrm{Fe})}\right)$ and pure liquid iron $\left(\Delta\mu_{\mathrm{Fe,ex}}^{(\mathrm{am})}\right)$ vs. milling time in the attritor

Theoretical Results and Discussion

For modeling it was assumed that the composition of Fe-based α-solid solution is constant and the composition of amorphous phase during AP was determined from the condition of mass balance (4). Calculations have shown that the composition of amorphous phase remains almost constant.

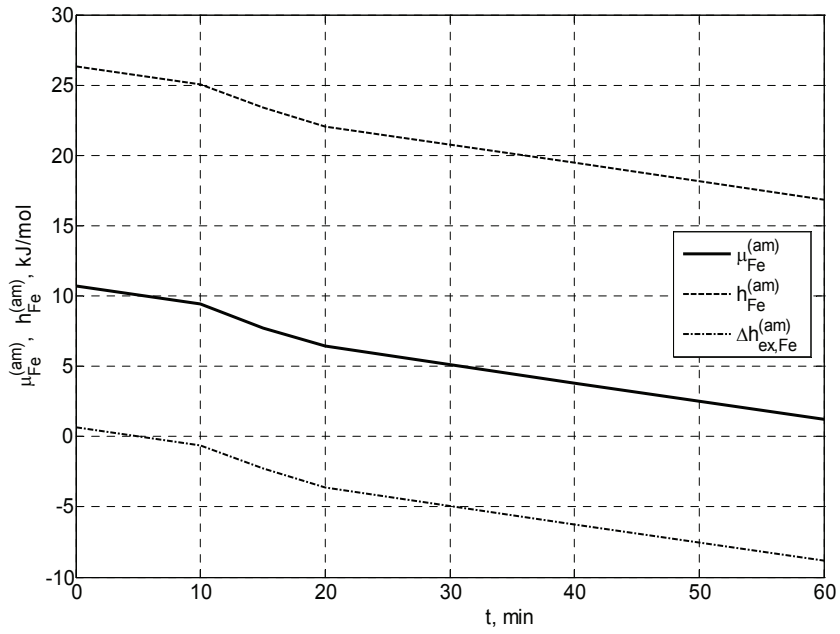

Fig. 1. Partial molar thermodynamic parameters of iron in the amorphous phase of alloy 1 vs. milling time in the attritor

For alloy 1, the chemical potential of iron in the amorphous phase $\mu_{\mathrm{Fe}}^{(\mathrm{am})}$, its partial molar enthalpy $h_{\mathrm{Fe}}^{(\mathrm{am})}$ and excess partial molar enthalpy $\Delta h_{\mathrm{ex,Fe}}^{(\mathrm{am})}$ at standard (room) temperature $T = 298$ K, which were calculated on the basis of the electrochemically measured values, are shown in Fig. 1 as functions of the processing time in the attritor. It is seen that increasing the AP duration brings about a noticeable decrease in the values of $\mu_{\mathrm{Fe}}^{(\mathrm{am})}$, $h_{\mathrm{Fe}}^{(\mathrm{am})}$ and $\Delta h_{\mathrm{ex,Fe}}^{(\mathrm{am})}$. Without AP $\Delta h_{\mathrm{ex,Fe}}^{(\mathrm{am})} > 0$, with increasing the milling time this value becomes negative. Therefore, during intensive plastic deformation of the material in the course of AP not only the dissolution of crystalline phases occurs but also the stability of amorphous phase improves.

Fig. 2 displays relative values of partial molar characteristics (chemical potential and enthalpy) of iron in the amorphous phase of alloy 1 with regard to crystalline phases: α-solid solution with the same composition as the amorphous phase $(\Delta\mu_{\mathrm{Fe}}^{(\mathrm{am}\to\alpha-\mathrm{ss})} = \mu_{\mathrm{Fe}}^{(\mathrm{am})} - G^{\alpha-\mathrm{ss}}$ and $\Delta h_{\mathrm{Fe}}^{(\mathrm{am}\to\alpha-\mathrm{Fe})} = h_{\mathrm{Fe}}^{(\mathrm{am})} - h_{\mathrm{Fe}}^{(\alpha-\mathrm{ss})})$ and pure α-Fe $(\Delta\mu_{\mathrm{Fe}}^{(\mathrm{am}\to\alpha-\mathrm{Fe})} = \mu_{\mathrm{Fe}}^{(\mathrm{am})} - G^{\alpha-\mathrm{Fe}}$ and $\Delta h_{\mathrm{Fe}}^{(\mathrm{am}\to\alpha-\mathrm{Fe})} = h_{\mathrm{Fe}}^{(\mathrm{am})} - H^{\alpha-\mathrm{Fe}})$. The excess

chemical potential of iron in the amorphous phase, $\Delta\mu_{Fe,ex}^{(am)} = \mu_{Fe,ex}^{(am)} - G_{Fe}^{liq}$, is also shown.

It is seen that the chemical potential of Fe in the amorphous phase is higher than the free energy of pure α-iron and substantially higher than its chemical potential in α-solid solution of the same composition, which is due to the non-equilibrium nature of amorphous phase. At the same time, it is more stable than pure liquid iron at room temperature because $\Delta\mu_{Fe,ex}^{(am)} < 0$. Parameter $\Delta\mu_{Fe}^{(am\to\alpha\text{-ss})}$ is a change in the chemical potential of Fe at diffusionless crystallization of the amorphous phase into supersaturated α-solid solution of the same composition while parameter $-\Delta h_{Fe}^{(am\to\alpha\text{-ss})}$ is actually the heat release during crystallization per 1 mole of iron in the solution.

The obtained results testify to the stabilization of amorphous phase as a result of intensive plastic deformation at AP. This can be attributed to a change in cluster-atomic structure of the quaternary amorphous phase [7].

The results of thermodynamic modeling of amorphous phase in alloy 2 are shown in Fig. 3 and 4.

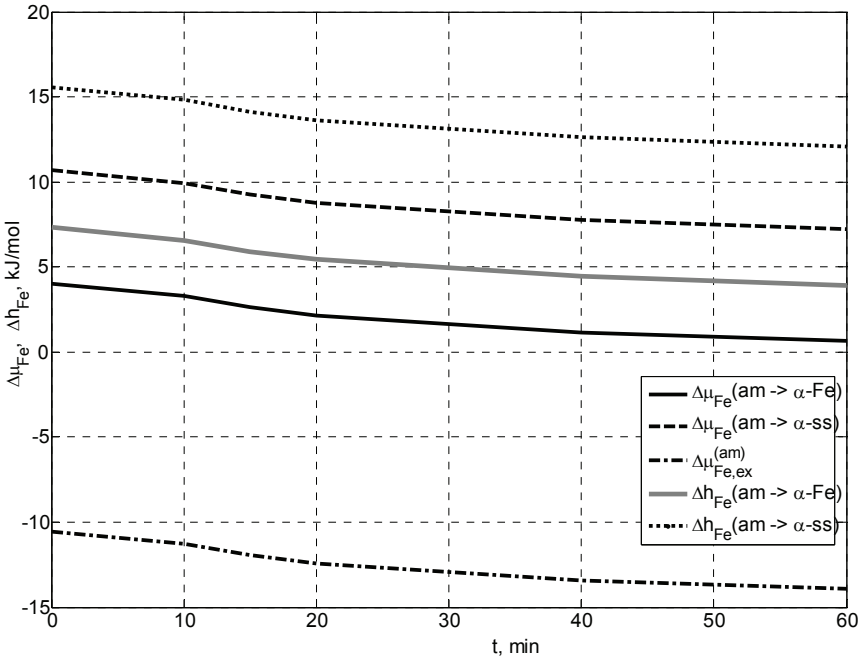

Fig. 4. Differences of partial molar thermodynamic parameters of iron in the amorphous phase of alloy 2 with regard to α-solid solution of the same composition $\left(\Delta\mu_{Fe}^{(am\to\alpha-ss)}\right.$ and $\left.\Delta h_{Fe}^{(am\to\alpha-ss)}\right)$, pure α-Fe $\left(\Delta\mu_{Fe}^{(am\to\alpha-Fe)}\right.$ and $\left.\Delta h_{Fe}^{(am\to\alpha-Fe)}\right)$, and pure liquid iron $\left(\Delta\mu_{Fe,ex}^{(am)}\right)$ vs. milling time in the attritor

At the qualitative level, in this system the dependence of the partial thermodynamic parameters of Fe in the multicomponent amorphous phase on the milling time is the same as in quaternary alloy 1 (compare Fig. 1 and 3). The difference is that the values of all the partial molar characteristics of iron in the amorphous phase are substantially lower than in alloy 1, the partial excess enthalpy $\Delta h_{ex,Fe}^{(am)}$ falls below zero at milling time $t > 10$ min and the excess chemical potential of Fe is negative for all milling times (Fig. 4). Thus, the multicomponent amorphous phase in alloy 2 appears to be more stable than the quaternary amorphous phase in alloy 1, and its stability is still increasing with intensive milling in an attritor.

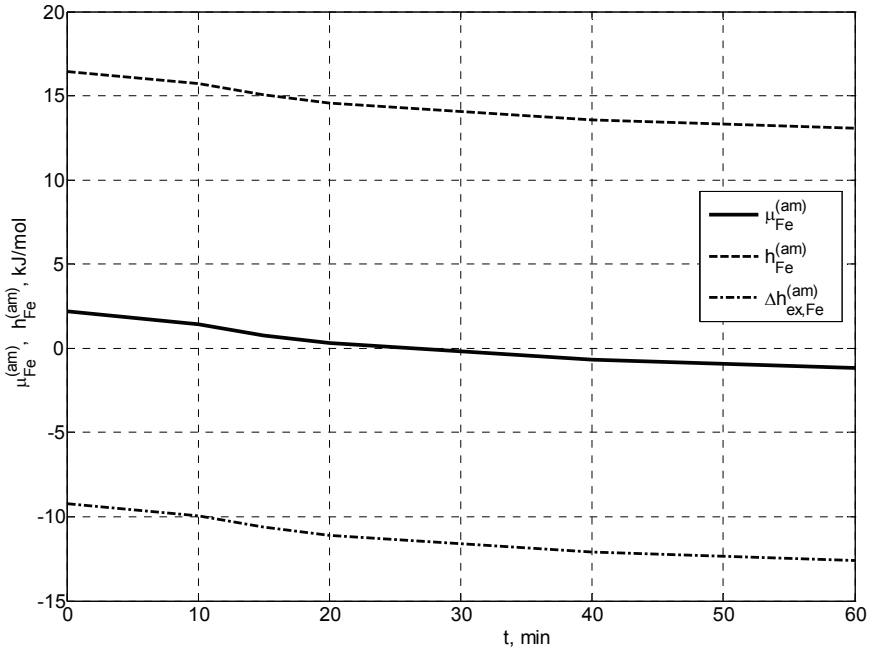

Fig. 3. Partial molar thermodynamic parameters of iron in the amorphous phase of alloy 2 vs. milling time in the attritor

Conclusion

A new thermodynamic model is developed for determining partial molar characteristics of a base metal (here Fe) of a multicomponent amorphous phase in a multiphase amorphous-crystalline alloy on the

basis of the results of electrochemical measurements. Calculations performed for two iron-base alloys have shown that the chemical potential of Fe and its partial molar enthalpy in the amorphous phase decrease during intensive ball milling in an attritor, that is the stability of the amorphous phase is substantially increasing. This is more evident for multicomponent alloy 2 (system Fe–Si–B–Ni–Co–Cr–Mo). Thus, complex alloying of iron with six elements combined with AP after melt quenching permits producing almost fully amorphous alloy that features good thermodynamic stability.

The developed thermodynamic method combined with experimental measurements can be used to characterize quantitatively the structural relaxation of amorphous alloys during annealing at a temperature below the crystallization point and to describe structural transformations that occur in amorphous phases at the cluster-atomic level at plastic deformation.

References

1. Elliott S.R. *Physics of Amorphous Materials*. Longman Group, 1983. 386 p.
2. A.M. Glezer. Creation principles of new-generation multifunctional structural materials. *Physics–Uspekhi*, 2012, vol. 55, no. 5, pp. 522-529.
3. Gallego L.J., Somoza J.A., Alonso J.A. Glass formation in ternary transition metal alloys. *Journal of Physics: Condensed Matter*, 1990, vol. 2, pp. 6245-6250.
4. Kutsenok I.B., Solomonova I.V., Tomilin I.A. Termodinamicheskaya stabil'nost' amorfnyh metallicheskih splavov [Thermodynamic stability of amorphous metallic alloys]. *Russian Journal of Physical Chemistry*, 1992, vol. 66, no. 12, pp. 3198-3204. (Rus)
5. Vasil'eva O.Ya., Kutsenok I.B., Tomilin I.A., Geydrih V.A. Termodinamicheskie svoystva amorfnyh splavov sistemy Co-Fe-Si-B [Thermodynamic properties of amorphous alloys of Co-Fe-Si-B system]. *Russian Journal of Physical Chemistry*, 1993, vol. 67, no. 6, pp. 1153-1155. (Rus)
6. Suryanarayana C. Mechanical alloying and milling. *Progress in Materials Science*, 2001, vol. 46, no. 1-2, pp. 1-184.
7. Greer A.L. Metallic glasses on the threshold. *Materials Today*, 2009, vol. 12, no. 1-2, pp. 14-22.
8. Inzelt G. Crossing the bridge between thermodynamics and electrochemistry. From the potential of the cell reaction to the electrode potential. *Chem Texts*, 2014, vol. 1, pp. 2-11.
9. Stolen S., Grande T., Allan N.L. *Chemical Thermodynamics of Materials: Macroscopic and Microscopic Aspects*. John Wiley & Sons, 2004. 398 p.
10. Lukas H.L., Fries S.G., Sundman B. *Computational Thermodynamics: The Calphad Method*. Cambridge University Press, 2007. 313 p.
11. Dinsdale A.T. SGTE data for pure elements. *Calphad*, 1991, vol. 15, pp. 317-425.
12. Miettinen J. Approximate thermodynamic solution phase data for steels. *Calphad*, 1998, vol. 22, pp. 275-300.
13. Liu Y.Q., Zhao X.S., Yang J., Shen J.Y. Thermodynamic optimization of the boron-cobalt-iron system. *Journal of Alloys and Compounds*, 2011, vol. 509, pp. 4805-4810.
14. Tokunaga T., Ohtani H., Hasebe M. Thermodynamic study of phase equilibria in the Ni-Fe-B system. *Materials Transactions JIM*, 2005, vol. 46, pp. 1193-1198.
15. Du Z., Guo C., Li C., Zhang W. Thermodynamic description of the Al-Mo and Al-Fe-Mo systems. *Journal of Phase Equilibria and Diffusion*, 2009, vol. 30, no. 5, pp. 487-501.
16. Poletti M.G., Battezzati L. Assessment of the ternary Fe-Si-B phase diagram. *Calphad*, 2013, vol. 43, pp. 40-47.
17. Liu Z.-K., Chang Y.A. Thermodynamic assessment of the Al-Fe-Si system. *Metallurgical and Materials Transactions A*, 1999, vol. 30, pp. 1081-1095.
18. Tomiska J. The system Fe-Ni-Cr: Revision of the thermodynamic description // *Journal of Alloys and Compounds*, 2004, vol. 379, no. 1-2, pp. 176-187.
19. Van der Kolk, A.R. Miedema, A.K. Niessen. On the composition range of amorphous binary transition metal alloys. *Journal of the Less-Common Metals*, 1988, vol. 145, pp. 1-17.
20. Takeuchi A., Inoue A. Calculations of mixing enthalpy and mismatch entropy for ternary amorphous alloys. *Materials Transactions JIM*, 2000, vol. 41, pp. 1372-1378.
21. Mansoori G.A., Carnahan N.F., Starling K.E., Leland T.W., jr. Equilibrium thermodynamic properties of the mixture of hard spheres. *Journal of Chemical Physics*, 1971, vol. 54, pp. 1523-1525.